

## IN VITRO STUDIES ON PMMA-BIOGLASS COMPOSITE FILMS

Laura FLOROIAN<sup>1</sup> and Attila BOER<sup>2</sup>

### Abstract

We report on the transfer of novel PMMA-bioglass composites by matrix assisted pulsed laser evaporation to uniform thin layers onto chemically etched Ti. The targets were prepared by freezing in liquid nitrogen after dissolution in chloroform mixtures containing PMMA reinforced with bioglass powders. The cryogenic targets were submitted to multipulse ablation with an UV KrF\* ( $\lambda = 248$  nm,  $\tau \sim 25$  ns) excimer laser source. The fluence was set after optimization at  $0.55 \text{ J} \cdot \text{cm}^{-2}$ .

We evaluated the films' bioactivity by immersion into simulated body fluid. The composition was monitored by Fourier transform infrared spectrometry and the morphology was monitored by confocal scanning laser microscopy.

*PACS:* 79.20.Ds, 87.85.jj.

*Key words:* bioactive materials, matrix assisted pulsed laser evaporation, confocal scanning laser microscopy.

## 1 Introduction

Due to the fact that many diseases/malfunctions of tissues and organs and other medical conditions cannot be healed or even treated successfully by conventional medical procedures, the field of biomaterials has developed tremendously over the last years. Healthcare consumers nowadays need increasingly advanced devices for diagnosis and treatment. New materials and innovative procedures and protocols to speed up osseointegration and subsequent bone repair and healing need to be developed.

Among the biomaterials with great potential we emphasize the newly formulated bioglasses and their composite which are capable of interacting with living materials and can be used in implantology and bone repair applications. In bulk the bioglasses brittle so that they are used as coatings for metallic implants. Metals are mechanically suitable for load-bearing orthopedic and dental implants, but, nevertheless, various problems related to corrosion, wear, and negative tissue interactions have been reported [1]. The coating of metallic implants with thin layers of bioactive material combines mechanical advantages with excellent biocompatibility. Furthermore, the coatings can protect the implants from corrosion, limiting the release of metallic ions into the body [2, 3, 4, 5].

---

<sup>1</sup>Faculty of Technological Engineering, *Transilvania* University of Braşov, Romania, e-mail: lauraf@unitbv.ro

<sup>2</sup>Faculty of Technological Engineering, *Transilvania* University of Braşov, Romania, e-mail: boera@unitbv.ro

In this study we investigate the possibility of using bioresorbable and bioactive composite made from polymethyl methacrylate (PMMA) and bioactive glass BG for implants or prosthesis for bone restoration and dental surgery. This new material is tested from the point of view of bioactivity and that of mechanical properties.

## 2 Materials and methods

Polymethyl methacrylate –  $(C_5O_2H_8)_n$  – is the synthetic polymer of methyl methacrylate and it is a transparent plastic often used as an alternative to glass because of its moderate properties, easy handling and processing and low cost. PMMA has a density of 1.150–1.190 kg/m<sup>3</sup>. This is less than half the density of glass, and similar to that of other plastics and of human bone. PMMA has a good impact strength higher than that of glass or polystyrene. It has excellent environmental stability compared to other plastics such as polycarbonate.

Unfortunately PMMA is softer and more easily to be scratched than glass. We want to obtain scratch-resistant coatings by the addition of the bioglass particles which besides have the ability to chemically bond to both bone and soft tissue (are bioactive).

In experiments we used bioglasses further denoted BG that contained 56.5% SiO<sub>2</sub>, 11% Na<sub>2</sub>O, 3% K<sub>2</sub>O, 15% CaO, 8.5% MgO, 6% P<sub>2</sub>O<sub>5</sub>. PMMA was dissolved in chloroform (percent of 3% PMMA) and into this solution the bioglass (0.5 %) in suspension was introduced. This mixture was frozen and maintained to a constant temperature and it served as targets in thin layer deposition which was made using the matrix assisted pulsed laser evaporation technique (MAPLE).

An excimer laser is used (KrF\* at 248 nm) with 25 ns pulse width, at 10 Hz repetition rates, focused to a 16 mm<sup>2</sup> spot size on the target. The best regime of deposition was identified for the following conditions: 0.55 J/cm<sup>2</sup> laser fluence,  $2 \cdot 10^{-2}$  torr pressure, 30 °C substrate temperature, 3 cm target-substrate distance and for the deposition of each film, we applied 12500 subsequent laser pulses. Once frozen, the MAPLE target is mounted on a cryogenically cooled rotating target holder with the open die end facing the laser. Once the chamber is evacuated, the target is cooled to 100 K temperature. We used medical grade Ti chemically etched as substrate because titanium is the most popular choice for the fabrication of orthopedic implants where high strength is required thanks to its good biocompatibility and very good mechanical characteristics.

## 3 Film characterization

We characterized the obtained films by confocal scanning laser microscopy (CSLM) and Fourier transform infrared spectrometry (FTIR). The morphological investigation process by using CSLM is based on a sequential exploration of a sample by a laser beam and on the monitoring of interaction effects between light and material for surface or spatial imaging. We used a Leica TCS SP system equipped with a He-Ne laser source (632.8 nm) and a PL Fluotar (40X magnification, numerical aperture NA = 0.7) objective. The images were recorded in reflection mode. Data processing and displaying were performed

by Leica software. FTIR analyses were conducted using a Nicolet 380 apparatus equipped with an orbit ATR (diamond crystal), wavenumber range  $7800 - 350 \text{ cm}^{-1}$ , spectral resolution  $0.4 \text{ cm}^{-1}$ , S/N ratio 20000:1. The spectra were taken in the absorbance mode. The bioactivity of the films was assessed in vitro by soaking the composite material films into simulated body fluid (SBF) followed by FTIR spectroscopic analysis to determine the extent of hydroxyapatite formation on the bioactive surface. The SBF was prepared by the mixing sodium chloride, sodium bicarbonate, potassium chloride, potassium phosphate, calcium chloride, dibasic potassium phosphate, hydrogen chloride, sodium sulfate and tris(hydroxymethyl)aminomethane into de-ionized water, according to Kokubo prescription [6]. The obtained solution had ionic concentration equal to human plasma. Table I compares the ionic concentrations of SBF with that of blood plasma.

Composition	Na <sup>+</sup>	K <sup>+</sup>	Mg <sup>2+</sup>	Ca <sup>2+</sup>	Cl <sup>-</sup>	HPO <sub>4</sub> <sup>2-</sup>	SO <sub>4</sub> <sup>2-</sup>	HCO <sub>3</sub> <sup>-</sup>
SBF concentration (mM)	142	5	1.5	2.5	147.8	1	0.5	4.2
Blood plasma composition (mM)	142	5	1.5	2.5	147.8	1	0.5	4.2

Table 1: Comparison of ionic concentrations of SBF and blood plasma.

The disks coated with sintered bioactive films were tested by immersion into 25.0 mL SBF preheated and maintained at  $37 \text{ }^\circ\text{C}$ . Tests are conducted after immersion from about 1 day to 2 weeks' immersion.

## 4 Results and discussions

### 4.1 Evaluation of bioactivity

We investigated bioactivity for two types of BG+PMMA films obtained from MAPLE targets which had a different PMMA/BG ratio: PMMA/BG=7.5 (named PMMA+BG 1) and PMMA/BG =5 (named PMMA+BG 2). The target for PMMA+BG 1 is made of 0.6 g PMMA reinforced with 0.08 g of 6P57 bioglass particles dissolved in 19.3 ml chloroform. For PMMA+BG 2 we used more bioglass.

Figure 1 makes a comparison between the FTIR spectra in absorbance mode for these PMMA+BG structures deposited by the MAPLE technique. The FTIR spectra perform different aspects. In the PMMA+BG 1 spectrum the peaks of PMMA prevail, such as a sharp intense peak at  $1721 \text{ cm}^{-1}$  due to the presence of ester carbonyl group stretching vibration, the broad peak ranging from  $1260-1000 \text{ cm}^{-1}$  owing to the C-O (ester bond) stretching vibration, the broad band from  $950-650 \text{ cm}^{-1}$  due to the bending of C-H. In the PMMA+BG 2 spectrum the peaks of BG prevail, such as the peaks at  $753 \text{ cm}^{-1}$ ,  $982 \text{ cm}^{-1}$  and  $1008 \text{ cm}^{-1}$  belonging to Si-O bending vibration modes.

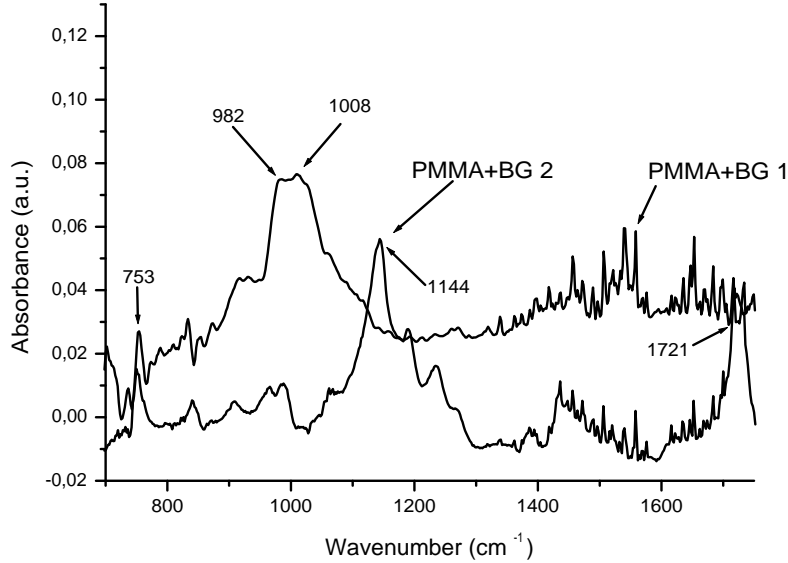


Figure 1: FTIR spectra of PMMA+BG 1 (bottom) and PMMA+BG 2 (top)

A lot of both PMMA+BG 1 and 2 samples were immersed into SBF and extracted one day, one week and two weeks later then analysed by FTIR. The sample presented a different behavior.

After one day's immersion into SBF solution, in the case of both PMMA+BG 1 and 2 samples, we can notice the growth of amplitude for all peaks (fig. 2) that indicates the forming of a rich superficial layer, where all elements have a greater concentration. This is consistent with other experimental observations made for bioglasses [7, 8] and it is accompanied by the loss of soluble silica into the solution, fact emphasized by the depreciation of the surface's quality observed by surface morphology analysis (see 4.2.).

After one week's immersion into SBF, the spectrum of PMMA+BG 1 samples does not change (fig 3(a)), while major transformations can be clearly noticed on the surface of the coatings PMMA+BG 2 (fig 3(b)): the bioglass peaks from  $982\text{ cm}^{-1}$  and  $1008\text{ cm}^{-1}$  decrease and a new peak appears, at  $1034\text{ cm}^{-1}$  that belongs to asymmetric stretching of P–O bond of  $(\text{PO}_4)^{3-}$ . This indicates diminishing silica concentration and appearance of the hydroxyapatite on surface coating.

Referring to fig. 5 in a typical FTIR scan of PMMA+BG 1 immersed for two weeks we could notice very little changes in the peaks' amplitude: peaks of PMMA+BG decreased –  $1144\text{ cm}^{-1}$ ,  $1722\text{ cm}^{-1}$  – and other peaks increased: at  $633$ ,  $960$ ,  $1076$ ,  $1470$ ; these little peaks are assigned of hydroxyapatite and indicate that the process of hydroxyapatite appearance is beginning.

On the other hand in the case of the PMMA+BG 2 coatings, the corresponding peaks

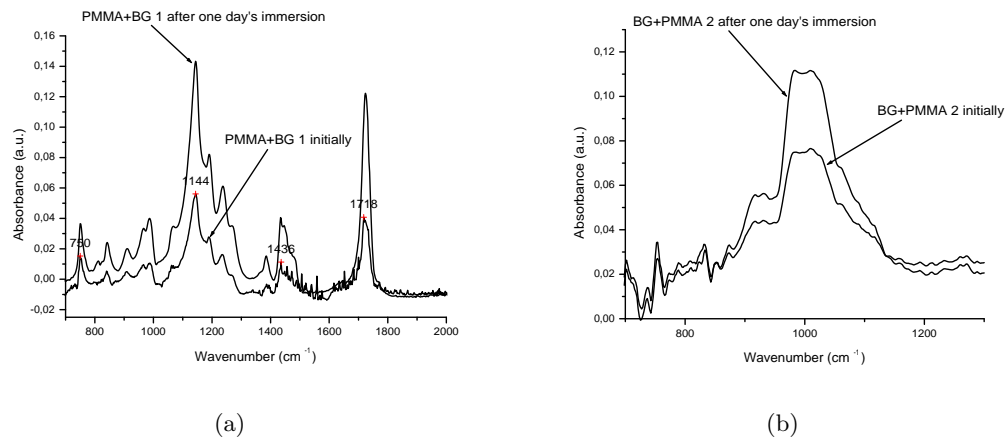


Figure 2: FTIR spectra of PMMA+BG1 (a) and PMMA+BG 2 (b) film before and after one day's immersion into SBF

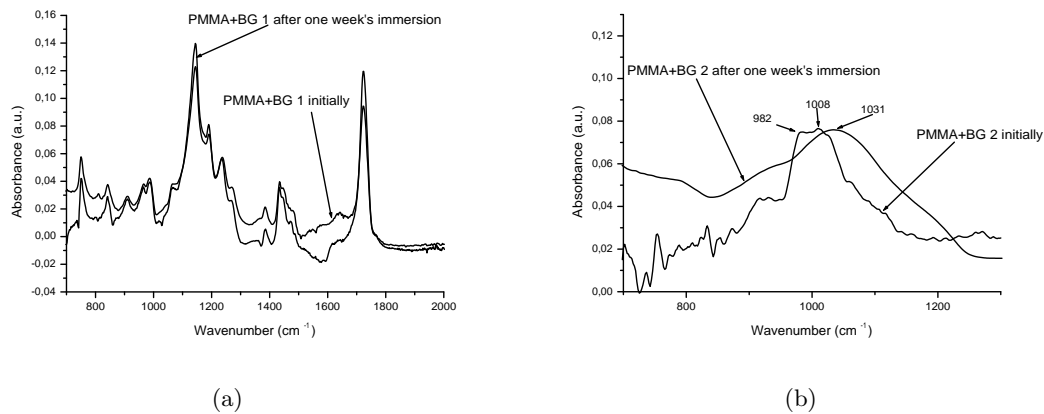


Figure 3: FTIR spectra of PMMA+BG1 (a) and PMMA+BG 2 (b) film before and after one week's immersion into SBF

for hydroxyapatite are well emphasized at 630, 865, 961, 1031 and 1090  $\text{cm}^{-1}$ . They correspond to the asymmetric (peaks at 1031 and 1090  $\text{cm}^{-1}$ ) and the symmetric (peak at 961  $\text{cm}^{-1}$ ) stretching of P–O bond in  $(\text{PO}_4)^{3-}$ , to  $(\text{HPO}_4)^{2-}$  replacing the  $(\text{PO}_4)^{3-}$  – peak at 865  $\text{cm}^{-1}$  and also to the librational mode of OH (peak at 630  $\text{cm}^{-1}$ ). At the same time the peaks' proper bioglass disappear.

These certify two things: the dissolution of the bioglass and the existence on the surface of a freshly growing carbonated hydroxyapatite  $\text{Ca}_{8.3}(\text{PO}_4)_{4.3}(\text{HPO}_4, \text{CO}_3)_{1.7}(\text{OH}, \text{CO}_3)_{0.3}$  which is the predominant mineral component of vertebrate bones. The growth of this layer demonstrates the ability of the material to achieve firmly bind to tissues a bioactive

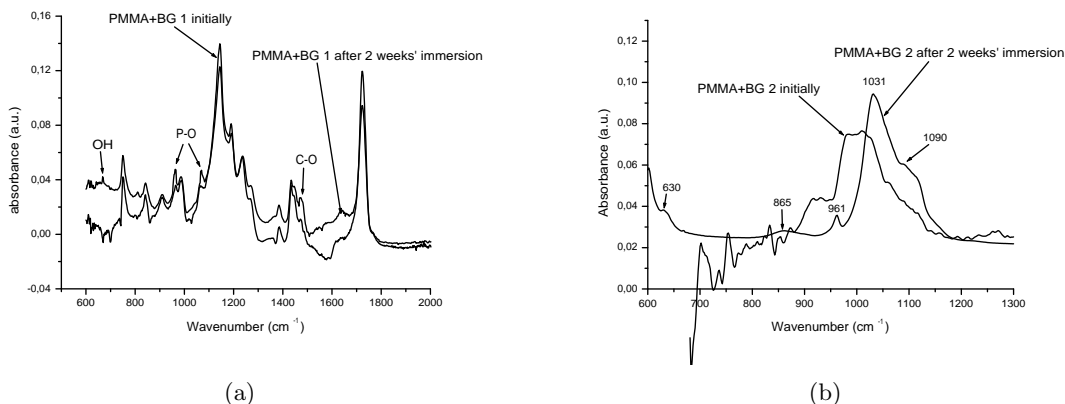


Figure 4: FTIR spectra of PMMA+BG 1 (a) and PMMA+BG 2 (b) film before and after two weeks' immersion into SBF

fixation through a chemical bond at the bone/implant interface. This behavior is similar to that reported for bulk glasses in the  $\text{SiO}_2 - \text{Na}_2\text{O} - \text{K}_2\text{O} - \text{CaO} - \text{MgO} - \text{P}_2\text{O}_5$  system, immersed into SBF [7, 9, 10, 11], and it is in accordance with the mechanism of apatite formation described by Hench for bioglasses [8]. The proposed subsequent steps were: i) the exchange of  $\text{Na}^+$  and  $\text{K}^+$  from glass with  $\text{H}^+$  or  $\text{H}_3\text{O}^+$  from SBF, accompanied by the loss of soluble silica into the solution and the formation of silanols ( $\text{Si} - \text{OH}$ ) on the glass surface; ii) condensation and repolymerization on surface of the  $\text{SiO}_2^-$ -rich layer; iii) migration of  $\text{Ca}^{2+}$  and  $\text{PO}_4^{3-}$  through the silica-rich layer forming a  $\text{CaO} - \text{P}_2\text{O}_5$ -rich film that incorporates calcium and phosphates from solution, and iv) the crystallization of the amorphous calcium phosphate film to form an apatite layer.

However the bioactivity of material is lower than that of pure bioglass BG films [12, 13] where the growing carbonated hydroxyapatite begins earlier, after a few days of immersion. PMMA additions reduce the bone bonding ability of bioactive glasses; this is in agreement with the studies of the effect of other materials introduction in bioactive glasses published by Ohura et al. [14] and Anderson et al. [15]. PMMA+BG 2 films have more bioglass than PMMA+BG 1 and are more bioactive; for BG+PMMA 2 films a hydroxyapatite layer is partially formed after one week's immersion into SBF, while for PMMA+BG 1 it is not visible until after the two weeks of immersion.

## 4.2 Surface morphology of PMMA+BG films

Afterwards, we have examined carefully the surface morphology of PMMA+BG 2 bioactive films before and after one week and two weeks' immersion into simulated body fluid.

3D image of titanium substrate (fig. 5(a)) revealed the structure with a characteristic configuration, consisting of a great number of irregularities and having  $3.101 \mu\text{m}$  root mean square.

The coating deposited from cryogenic targets of PMMA+BG 2 on the titanium sub-

strate preserved its morphology (fig. 5(b)) but the film surface had greater irregularities and its root mean square became  $\text{RMS}=3.813 \mu\text{m}$ , a value suitable for orthopedic applications, knowing the fact that for these the perfect roughness is less than 1 millimeter. Such feature favors biocompatibility which significantly increases with the specific area of the deposited biofilms. Indeed, the rougher the area due to surface protuberances, the higher the proliferation of viable cell cultures is [16, 17].

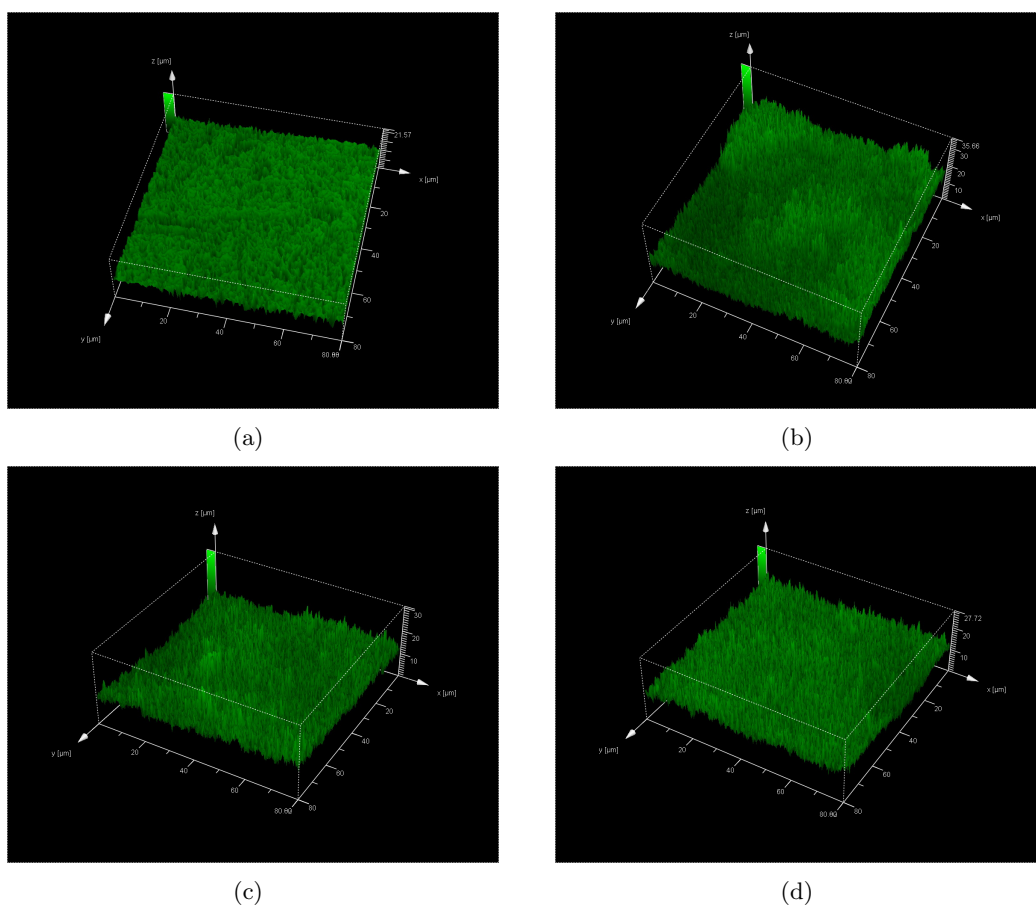


Figure 5: 3D images (40X magnification, 0.7 aperture, zoom 3.12) for: a) titanium substrate , b) PMMA+BG 2 initial film c) PMMA+BG 2 film after 1 week's immersion into SBF, d) PMMA+BG 2 film after 2 weeks' immersion into SBF

After one week's immersion the bioglass from bioactive film was dissolved in SBF and the roughness surface decreased down to  $\text{RMS}=2.726 \mu\text{m}$ . Thus 3D image (fig. 5(c)) and topographical image (fig. 6(c)) support observations by FTIR (fig. 3(b)).

FTIR analyzes certify the continuation of the bioglass dissolution and the appearance on the surface of a freshly growing carbonated hydroxyapatite after two weeks' immersion into SBF and CLSM confirms these affirmations: in figures 5(d) and 6(d) we can see new particles of variable size in the micrometric range that are randomly distributed over the

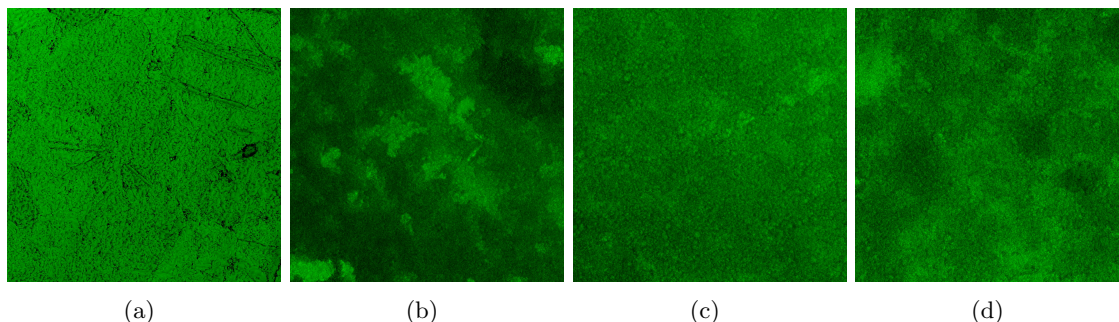


Figure 6: Topography (40X magnification, 0.7 aperture, zoom 1) for: a) titanium substrate, b) PMMA+BG 2 initial film c) PMMA+BG 2 film after 1 week's immersion into SBF, d) PMMA+BG 2 film after 2 weeks' immersion into SBF.

whole investigated area. Surface roughness still diminishes and becomes  $RMS=2.308 \mu m$ .

One advantage of PMMA+BG structure over bioglass films which makes it so great for implantology is that PMMA does not dissolve in SBF but it remains on the substrate and in this way implant corrosion and the release of metallic ions into the body are prevented. At the same time the structure preserves the bioglass bioactivity.

## 5 Conclusions

We have reported the performance of PMMA+BG thin films by the matrix assisted pulsed laser evaporation technique, deposition made with the preservation of the basic materials stoichiometry.

We have tested the obtained films in simulated body fluid solution and we have validated their bioactivity. When they are in contact with body fluids, the films present the ability to stimulate the growth of hydroxylapatite on their surface.

We can conclude that PMMA+BG compositions are suitable for being used as coatings on biological implants and they allow stable fixation to bone.

## References

- [1] Hench, L.L., Ethridge, E. C., *Biomaterials, An Interfacial Approach*, Academic Press, New York, 1982.
- [2] Hench, L. L., Anderson, O., *Bioactive glass coatings*, In: Hench LL, Wilson J, editors. An introduction to bioceramics. New Jersey: World Scientific, 239 1993.
- [3] Sousa, R.S., Barbosa, M. A., *Effect of hydroxyapatite thickness on metal ion release from Ti6Al4V substrates*, *Biomaterials* **17** (1996), 397–404.



- [4] Kokubo, T., Proceedings of the Third Euro-Ceramics, Faenza Editrice Iberica, San Vincente, vol. 3 (1993).
- [5] Santos, J.D., Silva, P.L., Knowles, J.C., Talal, S., Monteiro, F.J., *Reinforcement of hydroxyapatite by adding P2O5-CaO glasses with Na2O, K2O and MgO*, J. Mater. Sci., Mater Med., **7**(3) (1996), 187-189.
- [6] Kokubo, T., Kushitani, H., Sakka, S., Kitsugi, T., Yamamuro, T., *Solutions able to reproduce in vivo surface-structure changes in bioactive glass-ceramic A-W.*, J. Biomed. Mater. Res. **24**(6) (1990), 721-734.
- [7] Pazo, A., Saiz, E., Tomsia, A. P., *Silicate glass coatings on Ti-based implants*, Acta Mater, **46**(1998), 2551-2558.
- [8] Hench, L. L., *Bioceramics: from concept to clinic*, J. Am. Ceram.Soc., **74**, (1991), 1487-1570.
- [9] Ogino, M., Ohuchi, F., Hench, L.L., *Compositional dependence of the formation of calcium phosphate films on bioglass* J Biomed Mater Res **14** (1980), 55-64.
- [10] Hill, R., *An alternative view of the degradation of bioglass*, J Mater Sci Lett, **15** (1996), 1122-1125.
- [11] Gomez-Vega, J. M., Saiz, E., Tomsia, A. P., *Glass-based coatings for titanium implant*, J Biomed Mater Res **46** (1999), 549-559.
- [12] Floroian, L., Savu, B., Sima, F., Mihailescu, I.N., Tanaskovic, D., Janackovic, D., *Synthesis and characterization of bioglass thin films*, Digest Journal of Nanomat. And Biostrutures, **2**(3) (2007), 285-291.
- [13] Floroian, L., Savu, B., Stanciu, G., Popescu, A. C., Sima, F., Mihailescu, I. N., Mustata, R., Sima, L. E., Petrescu, S. M., Tanaskovic, D., Janackovic, D., *Nanostructured bioglass thin films synthesized by pulsed laser deposition: CSLM, FTIR investigations and in vitro biotests*, Applied Surface Science, **255** (2008), 3056-3062.
- [14] Ohura, K., Nakamura, T., Yamamuro, T., Ebisawa, Y., Kokubo, T., Kotoura, Y., Oka, M., *Bioactivity of CaO-SiO2 glasses added with various ions*, J Mater Sci, **3** (1992), 95-100.
- [15] Andersson, O.H., Karlsson, K.H., Kangasniemi, K., Yli-Urpo, A., *Models for physical properties and bioactivity of phosphate opal glasses*, Glastechn Ber **61** (1988), 300-305.
- [16] Eason, R., (Ed.), *Pulsed Laser Deposition of Thin Films: Applications-Lead Growth of Functional Materials*, Wiley & Sons, New York, USA, 2007.
- [17] Nelea, V., Morosanu, C., Iliescu, M., Mihailescu, I.N., *Hydroxyapatite thin films grown by pulsed laser deposition and RF magnetron sputtering: a comparative study*, Appl. Surf. Sci. **228** (2004), 346-356.

